3rd International Conference on New Developments in Soil Mechanics and Geotechnical Engineering,
28-30 June 2012, Near East University, Nicosia, North Cyprus

Numerical analysis of cross-walls effectiveness in reducing wall deflections associated to deep excavations

Efisio Erbì & Fabio M. Soccodato
University of Cagliari, Italy

KEYWORDS: cross-walls, deep excavations, ground movements, numerical analysis

ABSTRACT: This paper presents the main results of a three dimensional (3D) numerical study aimed to highlight the effects of length, span and stiffness of cross-walls (CWs) on their effectiveness. The 3D numerical analyses refer to a deep rectangular excavation, with excavation depths varying from 16 to 28 m. The soil profile is typical of the central area of Rome, and it is constituted by a thick soft clayey soil deposit covered by a top layer of coarse grained made ground. A *top-down* construction technique was assumed, in which floor slabs are realized after each excavation stage. Both diaphragm and cross walls were modelled with solid elements; thin solid interfaces were also introduced in order to correctly model the soil-wall and the wall-wall contacts. The results clearly showed that, depending on CWs span, CWs may be very effective in reducing wall and ground movements. For small CWs span almost plane strain conditions seem to apply, the global stiffness of the soil-structure system being controlled by the relatively high CWs stiffness; with increasing CWs span, wall deflections increase and 3D effects become more significant. The results also demonstrate that a CWs length a few meters greater than the final excavation depth is sufficient to generate an effective restraint to the embedded part of the retaining wall during the last excavation stage. The CWs stiffness does not appear to influence significantly the predicted wall movements.

1 INTRODUCTION

The design of deep excavations in the urban environment often requires the minimization of induced ground movements in order to avoid any significant effects of excavation on existing buildings and structures. It is well known that settlements induced by excavations are closely related to retaining wall deflections (Mana & Clough, 1981; Clough & O'Rourke, 1990, Ou et al 1996)). So, by selecting appropriate construction techniques and sequences that are capable to limit wall deflections, ground movements induced by excavation can be also minimized.
To this aim, *top-down* techniques are frequently used; when maximum deflections are to be tightly limited, *top-down* techniques may be further combined with the adoption of structural and sacrificial inclusions, such as cross-walls and buttress walls (Ou et al 2011). Cross-walls (CWs) are relatively stiff walls, constructed before excavation stage inside the excavation area, connecting the two main diaphragm walls. Buttress walls, which do not extent from one to the opposite retaining wall, are less effective than CWs: the amount of restraint effect is in fact governed by stiffness e strength mobilized at the soil-buttress contact (Ou et al 2006).

This paper presents the main results of a three-dimensional (3D) numerical study aimed to the evaluation of the influence of some key factors, such as CWs span, length and stiffness, on CWs effectiveness in reducing wall deflections. Geometry of the parametric study, soil profile and modeling approaches are described in the following section; successively, the numerical results are presented and discussed.

2 LAYOUT OF NUMERICAL ANALYSES

The 3D numerical analyses described in this paper refer to an ideal rectangular excavation (width B=20 m and length L=80 m), with excavation depths, H_e, varying from 16 to 28 m; the retaining wall length was assumed equal to 40 m. The soil profile is typical of the central area of Rome, and it is constituted by a top layer of coarse grained made ground (*MG*), 10 m in thickness, followed by a thick (50 m) soft clayey soil deposit (*Ag*); stiff layers of gravel and overconsolidated clay are found underneath. Pore water pressure distribution is almost hydrostatic, with a water level located approximately 10 m below ground level. A *top-down* construction technique was assumed, in which floor slabs are realized after each excavation (4 m) stage.
The numerical analyses were carried out with the commercial finite element code PLAXIS 3D Foundations (Plaxis BV, 2006). Figure 1 shows some typical meshes used in this study: both rectangular (L=80m) and infinitely long excavation geometries was considered. Due to the high stiffness of gravel and overconsolidated clay layers, the fixed bottom of the mesh was located at a depth of 60 m. Symmetry conditions allow to model, for the full 3D analyses, only a quarter of the problem. In order to minimize border effects, meshes extend away from excavation boundaries more than 5 times the maximum excavation height (Robosky 2005, Ou & Shiau 1998); on ateral boundaries, horizontal displacements were prevented by rollers. Both diaphragm walls (DWs) and CWs are constituted by rectangular (2.5x1.0 m) panels, modelled with isotropic elastic solid elements. For reinforced concrete DWs and floor slabs a Young modulus E=30 GPa was assumed. Thin (10 cm) solid interfaces were introduced in order to correctly model the soil-wall and the wall-wall contacts. In the reference analyses, interfaces were modelled as isotropic elasto-plastic, with a Mohr-Coulomb strength rule: stiffness and strength properties were related to those associated to the surrounding soils, by means of a scaling factor R_{int}=0.7. In other analyses, higher values of stiffness and strength of the DWs-CWs interfaces were adopted. The floor slabs, 20 cm in thickness, were modelled as anisotropic shell elements (membrane behaviour). A Poisson's ratio ν=0.2 was assumed for all structural elements.
The CWs effectiveness was studied by varying their span (i_{cw}=5, 10, 20 and 40 m), length (L_{cw}= 29, 30, 31, 32, 36 and 40 m) and stiffness (E_{cw}= 7, 12 and 30 GPa).

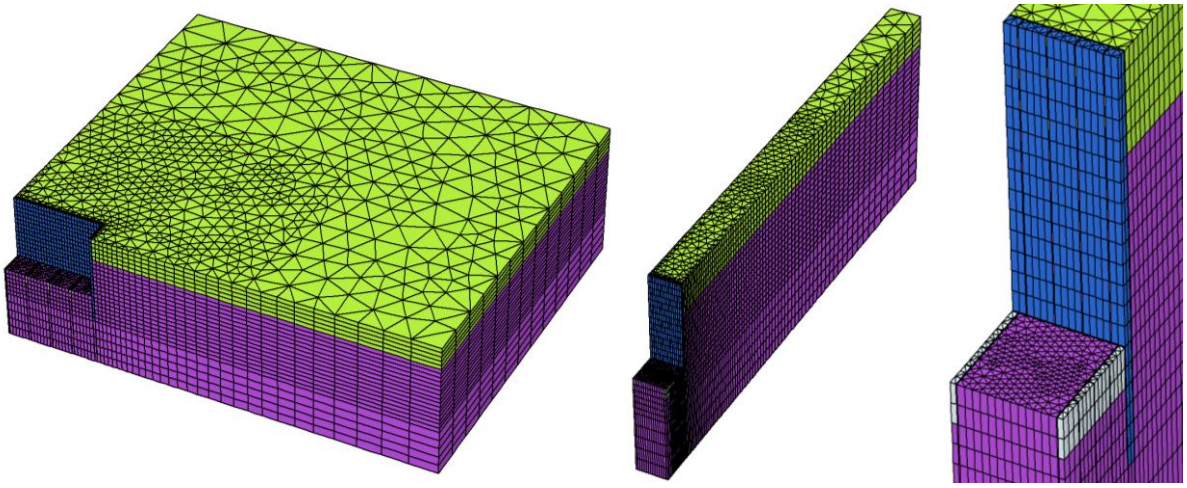

Figure 1 Typical meshes used in the analyses

The mechanical behaviour of soils was modelled with the Hardening Soil Model (Schanz et al. 1999), which is implemented in the finite element code. Table 1 and Table 2 show the model parameters used in the analyses. The calibration of model parameters follows from site geotechnical characterization. It should be noted that the elastic stiffness E_{ur} was set equal to the small strain stiffness observed in cross-hole, bender elements and resonant column tests, and high values of E_{ur}/E_{50} and E_{ur}/E_{edo} ratios were used to match the non-linearity of soil behaviour observed in laboratory tests. The dilatancy has been set equal to zero. More details on model calibration can be found in Erbì & Soccodato (2012).

Table 1. Hardening Soil model: general parameters

Soil	γ (kN/m^3)	c' (kPa)	φ' (°)	OCR (-)	K_0 (-)	ν' (-)
MG	18.5	15	28	2.0	0.50	0.2
Ag	18.2	20	25	1.3	0.58	0.2

Table 2. Hardening Soil model: stiffness parameters

Soil	E_{ur}^{ref} (MPa)	m (-)	$E_{ur}^{ref}/E_{50}^{ref}$ (-)	$E_{oed}^{ref}/E_{50}^{ref}$ (-)
MG	240	0.8	10.0	1.0
Ag	160	0.7	10.0	1.0

The analyses were carried out in terms of effective stresses, assuming that undrained conditions apply for the clay layer *Ag*. The steps of the analysis are the following: 1) initial conditions (geostatic stress state); 2) activation of diaphragm walls and CWs (wishes in place); 3) excavation step of 4 m; 4) installation of floor slab at the elevation reached before the excavation step; 5) Repetition of steps 3) and 4) until the final excavation depth (H_e=28 m) is reached.

3 ANALYSIS OF RESULTS

Figure 2 shows typical profiles of wall deflections u obtained for different CWs spans with increasing depth of excavation. The results are associated to the reference analyses, in which E_{cw}=12 GPa, L_{cw}=32 m and a soft interface (soil) was assumed to exists between DWs and CWs. Wall deflections shown in the figure are those computed in the section where maximum displacements occur (i.e., at the middle of CWs span); for direct comparison, the results of the analysis carried out in absence of CWs (no CW) are also plotted in the figure. The results clearly highlight the effects of CWs span in reducing wall deflections. It can be observed that, especially when looking at the final excavation stage, which also corresponds to the minimum CWs embedment (4 m, in this case), $i_{cw}\leq$10 m provides, immediately below excavation depth, a very effective restraint to the embedded part of the wall. Only very slight reductions of wall deflections are obtained by decreasing i_{cw}, while, as expected, for i_{cw}=40 m, wall deflections are close to those obtained in absence of CWs.
In Figure 3, with reference to the final excavation stage (H_e=28 m), the effects of CWs length are showed. It may be noted that only for the minimum CWs embedment (1 m) maximum deflections increase, especially for small CWs spans. With increasing L_{cw}, the restraint offered by CWs to the embedded part of DWs is more effective: it appears that CWs lengths greater than 32 m (i.e., 4 m below excavation depth) do not modify significantly wall deflection profiles.

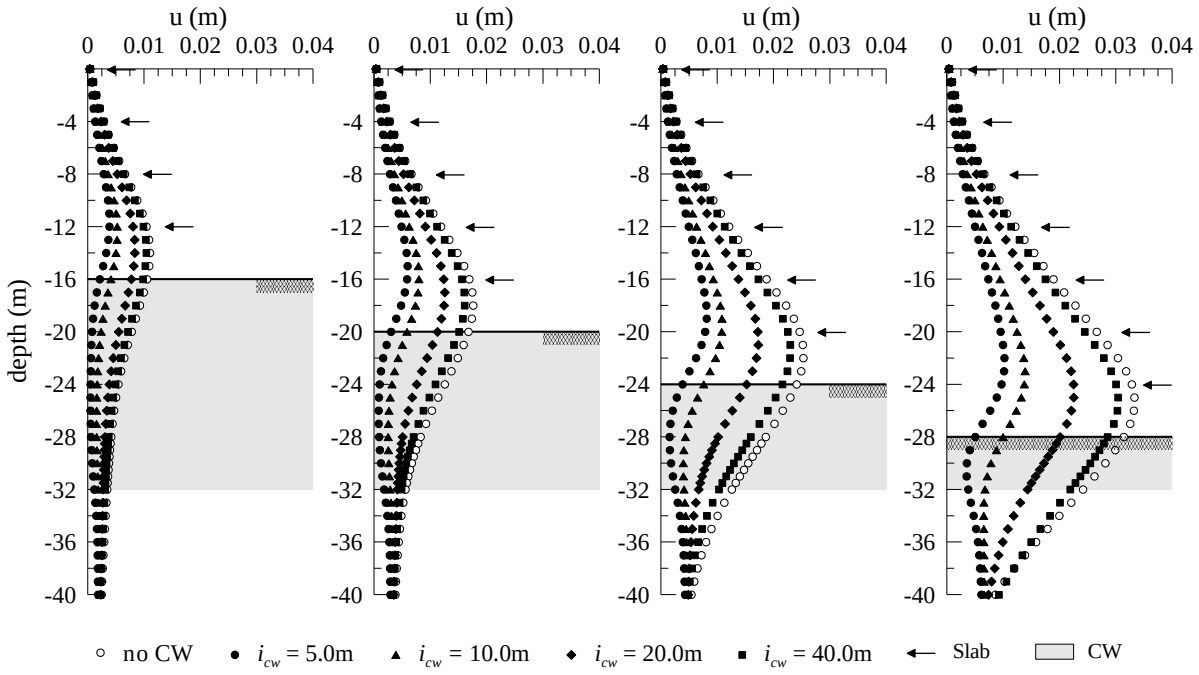

Figure 2 Maximum wall deflection: effects of CWs span (L_{cw}=32 m, E_{cw}=12 GPa).

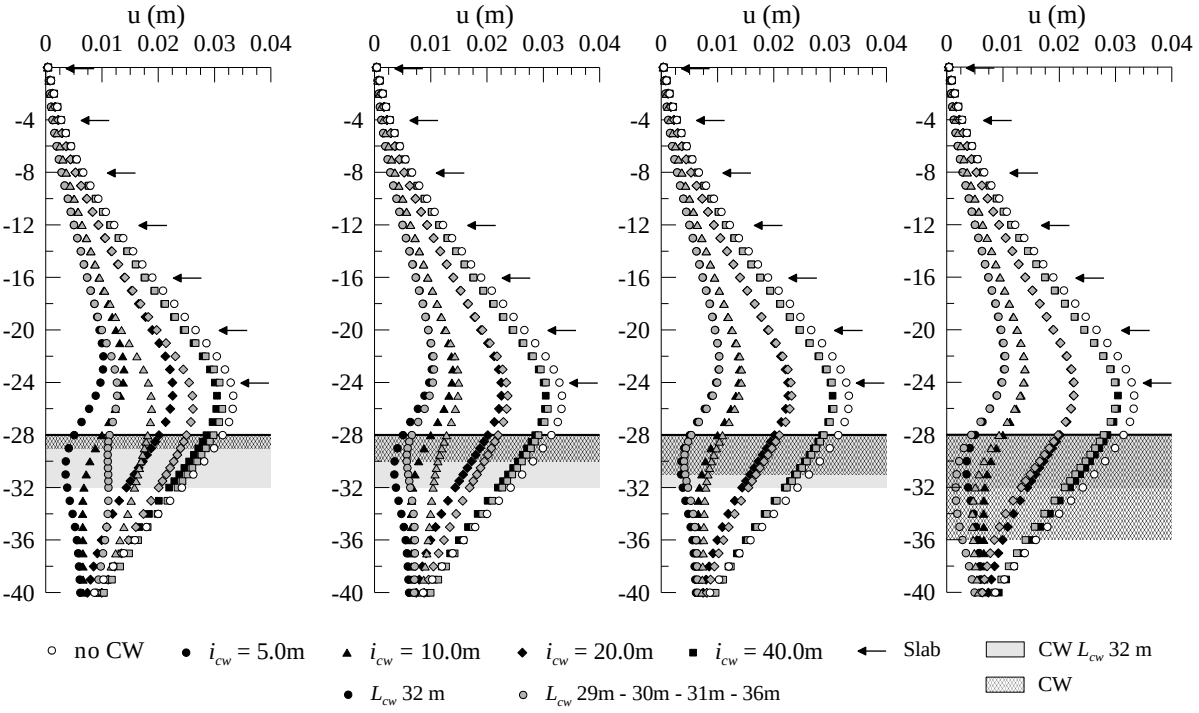

Figure 3 Maximum wall deflection: effects of CWs span and length (H_e=28 m, E_{cw}=12 GPa).

Horizontal displacement profiles related to the final excavation stage and laying on the horizontal plane on which maximum wall deflections occur are plotted in Figure 4. Apart from the corner effect, for i_{cw}=20 and 40 m a 3D behavior is clearly apparent, while for lower i_{cw} almost 2D plane strain conditions seem to apply. This occurrence may be attributed to the high stiffness of CWs as compared to the soil stiffness. In other terms, for low i_{cw} the system (soil-structure) stiffness is controlled by the CWs (elastic) stiffness while for high i_{cw} the soil stiffness (elasto-plastic) becomes more important.

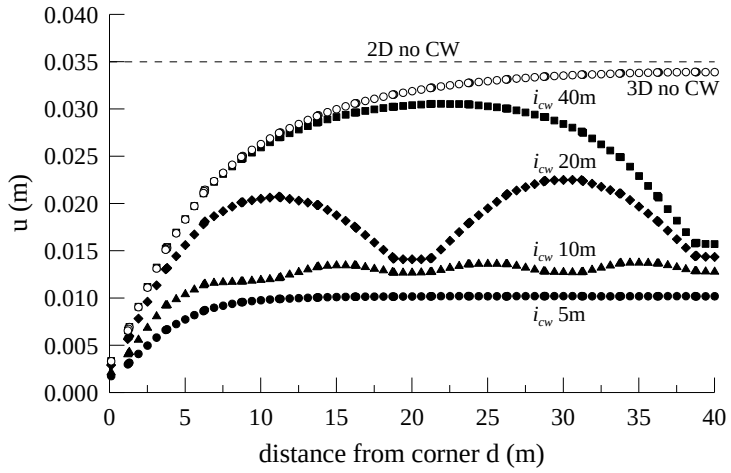

Figure 4 Wall deflections: effects of CWs span (H_e=28 m, L_{cw}=32 m, E_{cw}=12 GPa).

In all the cases under investigation, it may be noted from Figure 4 the significant contribution of CWs deformation to the total horizontal displacements of the wall. It was thus decided to carry out additional analyses by varying the stiffness of the soil interface between DWs and CWs and, also, the stiffness of the CW itself. Figure 5 shows that a 'rigid' connection between DWs and CWs allows to reduce, for i_{cw}=20 m, only for a 30% and 10% the CW and the maximum wall deflection, respectively. In the same figure, the horizontal displacements of a squared excavation, with B=L=20 m, are also plotted, assuming equal length and stiffness of DWs and CWs. Even though maximum displacements are similar, significant deformations of CWs are observed as compared to the corner effect restraint existing for the squared excavation.

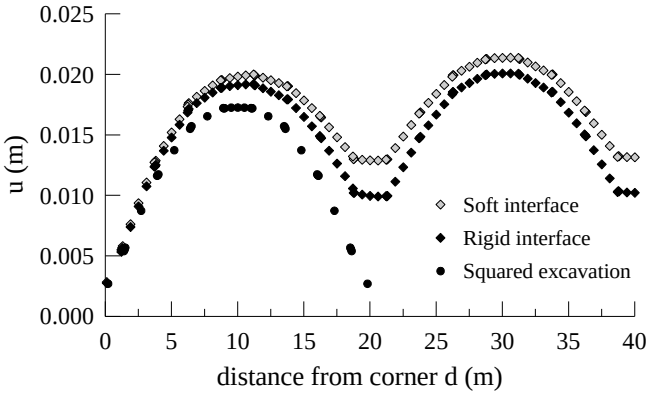

Figure 5 Wall deflections: effects of DWs-CWs interface stiffness (H_e=28 m, i_{cw}=20 m)

Finally, Figure 6 shows a summary of the results of the numerical analyses, linking the effectiveness of CWs, which is synthetically expressed by the ratio of maximum horizontal displacements in presence and absence of CWs, to CWs length, span and stiffness. As expected, CWs stiffness appears to have an effect similar to those above discussed when dealing with interface stiffness: by halving or doubling CWs stiffness, maximum displacements show a variation lesser than 10%. For the case under study, CWs embedment lengths below excavation line greater than 4 m give rise to identical CWs effectiveness.

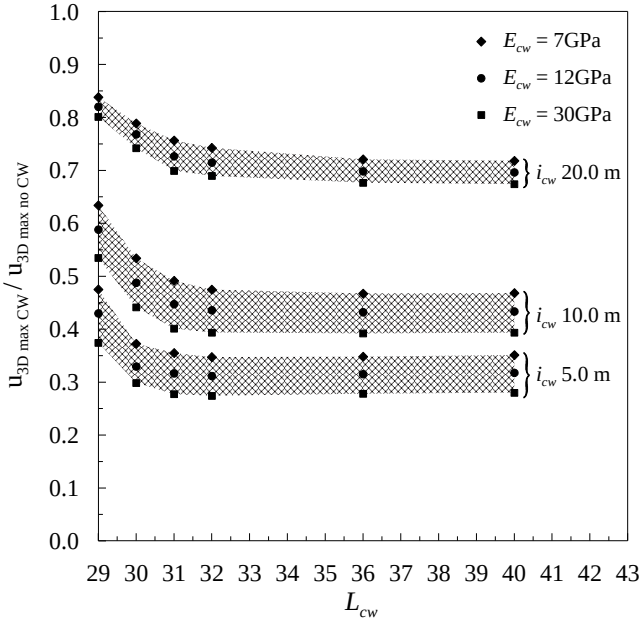

Figure 6 CWs effectiveness in reducing wall deflections

4 CONCLUSION

In this paper the main results of a 3D numerical study aimed to highlight the effects of length, span and stiffness of CWs on their effectiveness have been presented and discussed. The 3D numerical analyses refer to a deep rectangular excavation. The soil profile is constituted by a thick soft clayey soil deposit covered by a top layer of coarse grained made ground. An elasto-plastic with stress dependent stiffness and isotropic volumetric and deviatoric hardening model was used in order to simulate the high non–linear soil behavior. A top-down construction technique was assumed, in which floor slabs are realized after each excavation stage. Both DWs and CWs panels were modelled with solid elements; thin solid interfaces were also introduced in order to correctly model the soil-wall and the wall-wall contacts.

The results clearly showed that, depending on CWs span, CWs may be very effective in reducing wall and ground movements: for a CWs span equal to 10 m the maximum wall deflection is about 50% of that in absence of CWs. For small CWs span almost plane strain conditions seem to apply, the global stiffness of the soil-structure system being controlled by the relatively high CWs stiffness; with increasing CWs span, wall deflections increase and 3D effects become more significant. The results also demonstrate that, for the case under investigation, a CWs length a few meters greater than the final excavation depth is sufficient to generate an effective restraints to the embedded part of the retaining wall during the last excavation stage. The CWs stiffness does not appear to significantly influence the predicted maximum wall movements: a variation lesser than 10% was obtained by halving or doubling CWs stiffness.

REFERENCES

Clough G.W. & O'Rourke T.D. (1990). Construction induced movements of in situ walls, Proc. Design and performance of earth retaining structures, Ithaca, NY, ASCE GSP 25: 430-470.

Erbì E. & Soccodato F.M. (2012). A 3D numerical study of deep excavation in clayey soils, Proc 7Th Int. Symp. On Geotechnical Aspects of Underground Construction in Soft Ground, IS Rome 2011. (in print).

Finno R.J. & Roboski J.F. (2005). Three-Dimensional responses of a Tied-Back Excavation through clay, Journal of Geotechnical and Geoenviromental Engineering 131 (3): 273-282.

Hsieh H.S., Lu Y.C. & Lin T.M. (2008). Effects of joint details that on the behavior of cross walls, Journal GeoEngineering 3 (2): 55-60.

Mana A.I. & Clough G.W. (1981). Prediction of movements for braced cuts in clay, Journal Geotechnical Engineering Division, ASCE 107 (6): 759-777.

Ou, C.Y., Chiou, D.C. & Wu, T.S. (1996). Three-Dimensional finite element analysis of deep excavations. *Journal of Geotechnical Engineering*, 122 (5): 337-345.

Ou, C.Y. & Shiau, B.Y (1998). Analysis of the corner effect on excavation behaviors, Canadian Geotechnical Journal 35, 532-540.

Ou C.Y., Lin Y.L. & Hsieh P.G. (2006). A case record of an excavation with cross walls and buttress walls, Journal GeoEngineering 1 (2): 579-586.

Ou C.Y., Hsieh P.G. & Lin Y.L. (2011). Performance of excavation with cross walls, Journal of Geotechnical and Geoenviromental Engineering, ASCE 137 (1): 94-104.

Plaxis 3D Foundation, verison 1.6, Plaxis user manual, Delft University of Technology & Plaxis bv The Netherlands.Netherlands, 2006.

Schanz T., Vermeer P.A. & Bonnier P.G. (1999). Formulation and verification of the Hardening-Soil Model, In: R.B.J. Brinkgreve, Beyond 2000 in Computational Geotechnics. Balkema, Rotterdam: 281-290.

Wang J.H., Xu, Z.H. & Wang W.D. (2010). Wall and ground movements due to deep excavations in Shanghai soft soils, Journal of Geotechnical and Geoenviromental Engineering 136 (7): 985-994.